

Evolution of Oxygen-rich and Carbon Stars on the Asymptotic Giant Branch

Sun Kwok¹, Kevin M. Volk², and S. Josephine Chan¹

¹The University of Calgary, Calgary, Canada

²NASA Ames Research Center, Moffett Field, California, U.S.A.

I. Introduction

For many years, it has been commonly believed that oxygen-rich (M) stars evolve first to S stars and then to carbon (C) stars. However, the details of the transition are not understood. It is now accepted that the overabundance of carbon ($[C/O] > 1$) in some asymptotic giant branch (AGB) stars is due to the dredge up of products of α capture and s-process elements after a number of thermal pulses (Iben 1975). Effects of convective overshooting and semiconvection in the dredge up process have also been considered (Castellani *et al.* 1985, Lattanzio 1986). The dredge up of carbon into the photosphere leads to the formation of carbon-based molecules, which absorption bands become the basis of spectral classification.

During the past decade, it is recognized that the carbon-richness of a star not only manifests itself in the photospheric spectrum, but also in the circumstellar environment as well. Probes of the circumstellar envelopes in the infrared and radio regions provide new means to characterize the chemical properties of the star. These methods are particularly useful in cases where the photosphere is heavily obscured by circumstellar absorption. Table 1 summarizes the photospheric and circumstellar spectral characteristics of M and C stars.

Table 1

O-rich stars	C-rich stars
	Optical (photospheric)
TiO, VO	C ₂ , CN 3219 stars in GCCCS (Stephenson 1973).
	Infrared (circumstellar)
9.7 μ m silicate dust feature ~2000 objects in <i>IRAS</i> LRS classes 21-29, 31-39.	11.2 SiC dust feature 538 objects in <i>IRAS</i> LRS classes 41-49.
	Radio (circumstellar)
1612 MHz OH maser ~400 detected as of 1987	λ 2.6mm rotational transition of CO ~170 detected as of 1987, approximately half are from oxygen-rich stars.

While large numbers of stars have been classified optically as carbon stars (hereafter visual carbon stars) using, e.g. objective prism surveys, there have been an increasing number of carbon-rich objects which are discovered in infrared surveys, the most famous example being CW Leo (IRC+10°216).

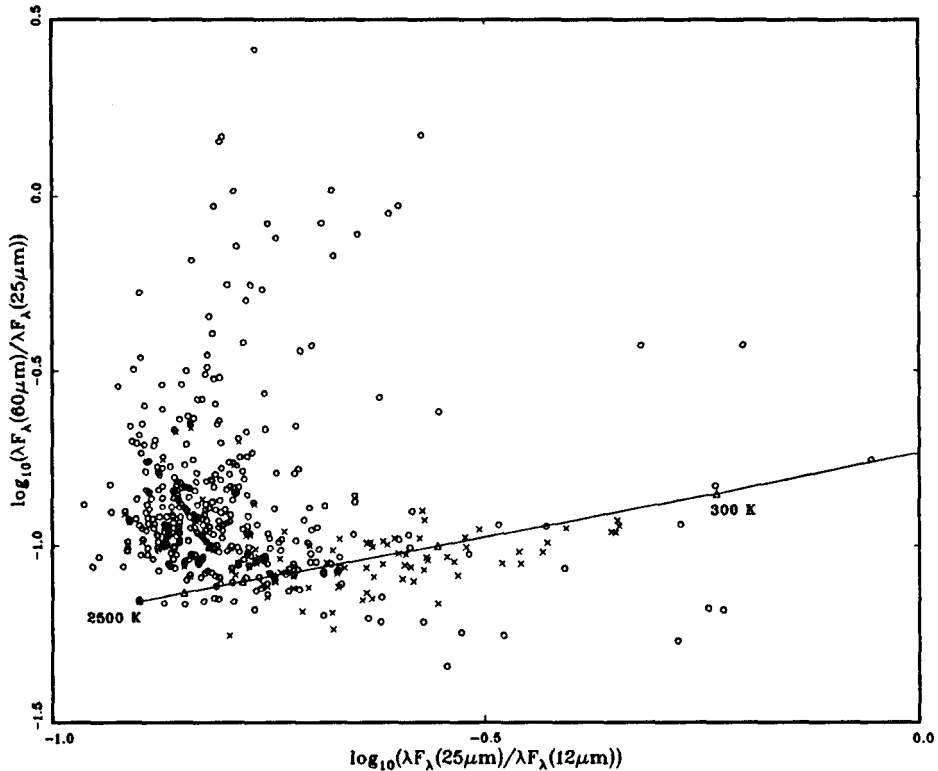


Figure 1. Color distributions of visual and infrared carbon stars. Circles: 386 visual carbon stars in GCCCS and MacConnell (1988) with good fluxes at 12, 25, and 60 μm *IRAS* bands; crosses: 111 stars in *IRAS* LRS classes 41-49 with good fluxes at all four *IRAS* bands.

CW Leo shows strong thermal emission line from the CO molecule, which suggests a carbon-rich nature. The Low Resolution Spectrometer (LRS) on *IRAS* has also discovered new objects which show the 11.2 μm silicon carbide feature, instead of the 9.7 μm silicate feature which is commonly observed in M stars. It is interesting to find that these infrared and radio carbon stars do not entirely overlap with the population of traditional visual carbon stars, and the inter-relationships between these three classes of carbon stars need to be clarified.

II. Color distributions of carbon stars

Many of the visual carbon stars were detected by *IRAS*. Figure 1 shows the distribution of 369 carbon stars in GCCCS and 17 southern carbon stars discovered by MacConnell (1988). Most of these objects have strong 60 μm excess, which was noted by Thronson *et al.* (1987). In contrast, radio carbon stars are found to cluster around the blackbody line (Zuckerman and Dyck 1986). Also plotted in Fig. 1 are 111 infrared carbon stars which are found to have the 11.2 μm SiC feature (Chan and Kwok 1988). Fig. 1 suggests that while visual, infrared, and radio carbon stars are all manifestation of carbon richness, they nevertheless occupy distinct parts of the color-color diagram.

III. Visual carbon stars as transition objects

The observed 60 μm excess and the detection of silicate feature in some visual carbon stars have led to the theory of Willems and deJong (1988) which proposes that visual carbon stars represent a transitional evolutionary phase after an interruption of mass loss during the Mira variable phase. As the oxygen-rich circumstellar shell disperses into the interstellar medium, the carbon-rich photosphere will be observed as a carbon star while emission from the remnant envelope contributes

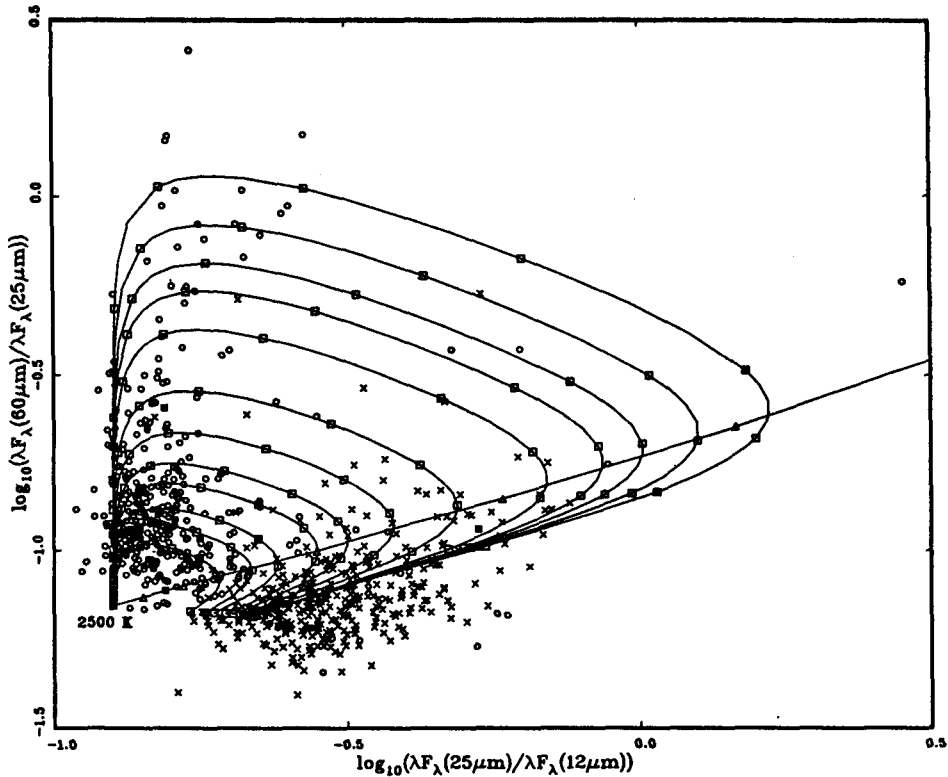


Figure 2. The evolutionary tracks for carbon stars on the color-color diagram. Also plotted are the visual carbon stars (circles) and M stars (crosses) showing the silicate feature in emission. The model tracks represent initial mass loss rates of 10^7 (inner most) to $10^5 M_{\odot} \text{ yr}^{-1}$ (outer most).

to the excess in far-infrared wavelengths. We have repeated the model calculations of Willems and deJong, while at the same time taking into account the effects of the silicate grain opacity function and temperature and density gradients in the circumstellar envelope. Model spectra were calculated for 12 initial mass loss rates (from 10^7 to $10^5 M_{\odot} \text{ yr}^{-1}$) at 35 different epochs after the termination of mass loss. This resulted in a total of 435 spectra which were then convolved with the *IRAS* instrumental profiles to simulate the photometry measurements. Figure 2 shows the model evolutionary tracks on the color-color diagram. We can see that the tracks start in the area of the color-color diagram populated by M stars and describe loops of various sizes which pass through most of the visual carbon stars. After $\sim 10^3$ yr, the tracks begin to turn downward and after $\sim 5 \times 10^4$ yr, the shell has effectively totally dispersed and the stellar color resembles that of the photosphere.

Many visual carbon stars have ground-based photometry which can be used for detailed comparison with the models. A total of 123 stars were fitted by Chan and Kwok (1988). Figure 3 shows an example of such fits. The initial mass loss rate and the time since shell detachment can be determined from the fitting process. The excellent agreement between the models and observations gives us confidence in the correctness of the detached shell model.

As new SiC grains are formed, the optical depth of the circumstellar envelope will increase again and the $11.2 \mu\text{m}$ feature will become more prominent. Figure 4 shows the spectrum of the infrared carbon star T Dra (LRSC 45) fitted by a radiative transfer model using a r^{-2} density distribution. We can see that the dust continuum emission is already important at $\lambda \sim 5 \mu\text{m}$. We suggest that T Dra represents an intermediate object between visual carbon stars and radio carbon stars like CW Leo where the color temperature is only ~ 500 K. The very high mass loss rates of stars like CW Leo will quickly deplete the hydrogen envelope, leading to the formation of a carbon-rich planetary nebula.

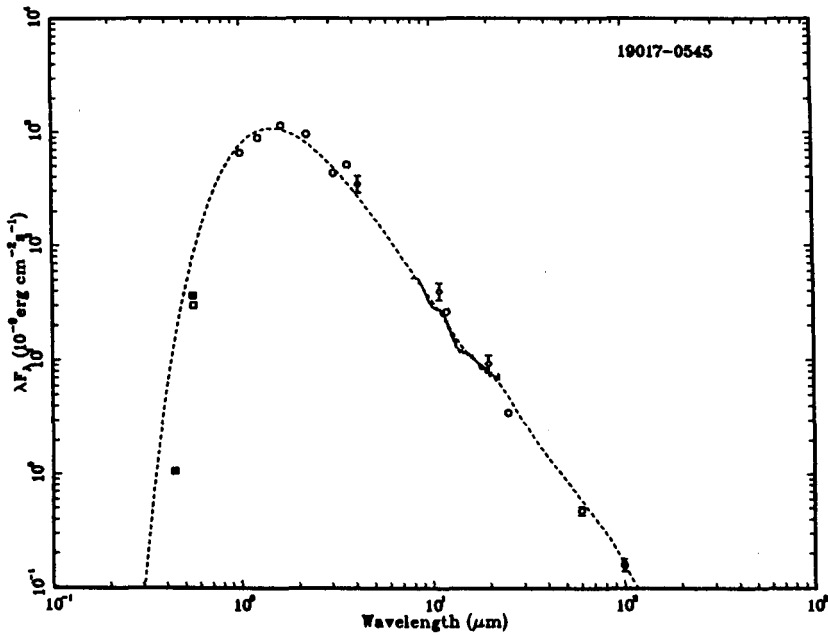


Figure 3. Model spectral fit to V Aql. The derived angular size of the inner radius is 0.7 arc sec and optical depth at 9.7 μm is 3.6(-3).

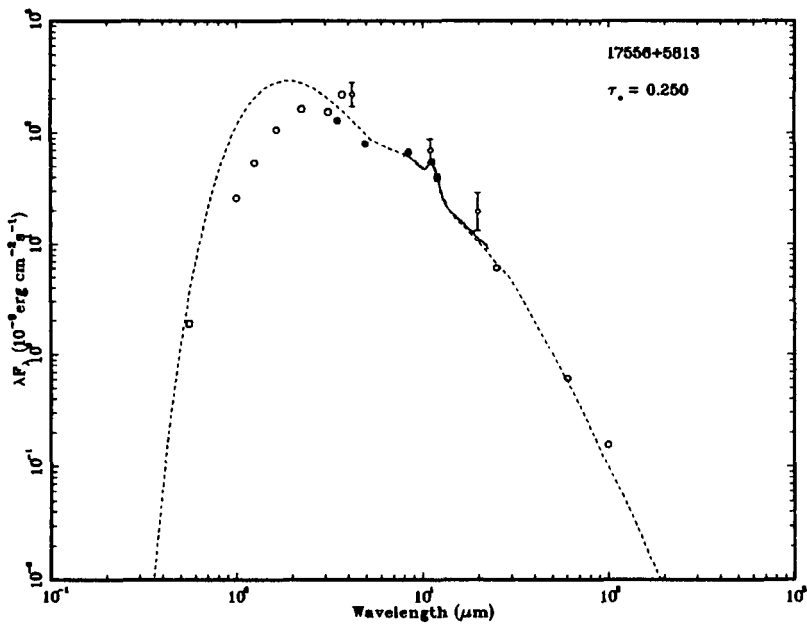


Figure 4. The spectrum of T Dra fitted by a radiative transfer model. The optical depth at 11.2 μm is 0.25.

IV. S stars

S stars show C/O abundance in between that of M and C stars and have often been suggested as transition objects between M and C stars. A cross-reference check of the General Catalogue of S Stars by Stephenson (1976) and the *IRAS* Point Source Catalog suggests that S stars belong to both LRS classes 21–29 (oxygen-rich) and 41–49 (carbon rich). S stars also do not possess unique colors but instead overlap extensively with both M and C stars in the color-color diagram. While S stars can be isolated through their photospheric spectra, we find no common infrared property which characterizes them as a separate group.

V. Radio observations of visual carbon stars

Recent CO observations have led to the detection of many visual carbon stars (Olofsson, Eriksson, and Gustafsson 1987, 1988). These detections confirm that visual carbon stars process extensive circumstellar envelopes as suggested by their 60 μm excess. Most interestingly, the carbon star S Sct was found to have a double-peaked CO profile, which is interpreted by Olofsson *et al.* (1988) as due to a detached shell. They estimate that the outer radius of the shell to be >140 arc sec. In comparison, model fitting of the infrared spectrum of S Sct by Chan and Kwok (1988) estimate an inner radius of 30 arc sec. An expansion velocity of 20 km s^{-1} implies that mass loss in S Sct terminated ~ 7000 (D/kpc) yr ago. The observation of the double-peaked profile therefore provides strong support that visual carbon stars are in between two mass-losing phases of evolution.

VI. Evolution of oxygen-rich stars on the AGB

While the above scenario may account for the evolution of carbon stars on the AGB, the observations of M stars with very deep silicate absorption features suggest that the optical depth of the circumstellar envelope must be very high ($\tau \sim 50$ at 9.7 μm). The corresponding mass loss rates have to be $>10^5 M_{\odot} \text{ yr}^{-1}$. With such high mass loss rates, the lifetime of such objects must be very short, probably $<10^3$ yr. It is therefore unlikely that these objects will evolve to, or have evolved from, carbon stars. A reasonable hypothesis is that there is a branching on the AGB, where some stars evolve into carbon stars as described in §III, while others remain oxygen-rich.

The fact that OH/IR stars occupy a well-defined band on the color-color diagram was first noted by Olton *et al.* (1984). Figure 5 shows a plot of the silicate emission (LRSC 25–29) and absorption (LRSC 31–39) objects on the color-color diagram. The difference in colors of these two groups of objects suggests that stars change from emission to absorption objects as the mass loss rate increases while they ascend the AGB. The band on the color-color diagram can therefore be interpreted as an evolutionary sequence (Bedijn 1987, Volk and Kwok 1988).

Since the remnant of the dust circumstellar envelope created during the AGB should still be present during the planetary nebula phase, planetary nebulae should be far infrared emitters (Kwok 1980). Approximately 1000 planetary nebulae were in fact detected by *IRAS* (Pottasch *et al.* 1984). The color distribution of 126 planetary nebulae is also shown in Fig. 5. These planetary nebulae are selected based on their high radio brightness temperature (T_b):

$$T_b(5\text{GHz}) = (c^2/2\pi k\nu^2)(F_{\nu}/\theta^2) \quad (1)$$

where F_{ν} is the 5 GHz flux and θ is the angular radius of the nebula. T_b is a convenient parameter to use not only because it can be readily determined by observations, but also because it is distance independent. As the surface brightness of planetary nebulae is expected to decrease as a result of expansion, T_b is therefore also an age indicator. The observed range of T_b in planetary nebulae is between 0.1 K to 10,000 K, and the 126 nebulae selected here probably represent the younger members of planetary nebulae. We find that the infrared colors of these high surface brightness objects to be less affected by atomic line emission than more-evolved planetary nebulae. There are also indications in Figure 5 that the nebulae with $T_b > 1000$ K have higher color temperatures than the nebulae with T_b between 100 and 1000 K.

Also shown in Fig. 5 are evolutionary tracks for two stars with initial masses 1.5 and 8 M_{\odot} on the color-color diagram based on the model calculation of Volk and Kwok (1988). The break points (point A) of the tracks represent the tip of the AGB, where mass loss is assumed to terminate. The ends of the tracks (point B) represent approximately 300 and 1300 yr after the end of AGB for the 1.5 and 8 M_{\odot} cases respectively. Between points A and B, the circumstellar envelope is dispersing into the interstellar medium and physically detached from the star. These tracks successfully simulate the change in color of AGB stars, and also seem to be extending to the area of the color-color diagram

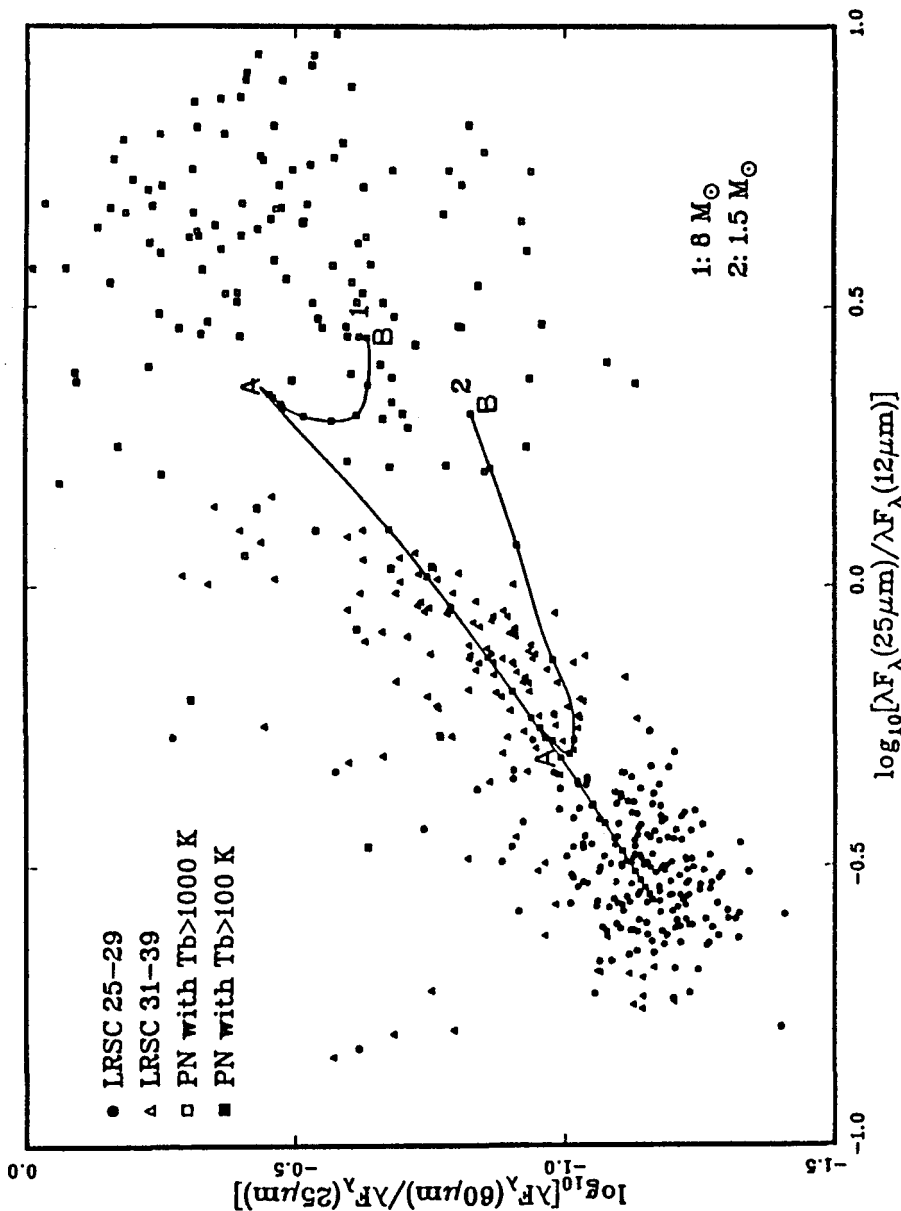


Figure 5. The evolutionary tracks for stars of masses 8 and 1.5 M_{\odot} on the color-color diagram. The tracks originate from the area populated by AGB stars showing silicate emission features (circles), move upward through the area occupied by silicate absorption objects (triangles), and after the termination of mass loss (point A), shift to the right toward the area occupied by planetary nebulae (squares).

occupied by planetary nebulae.

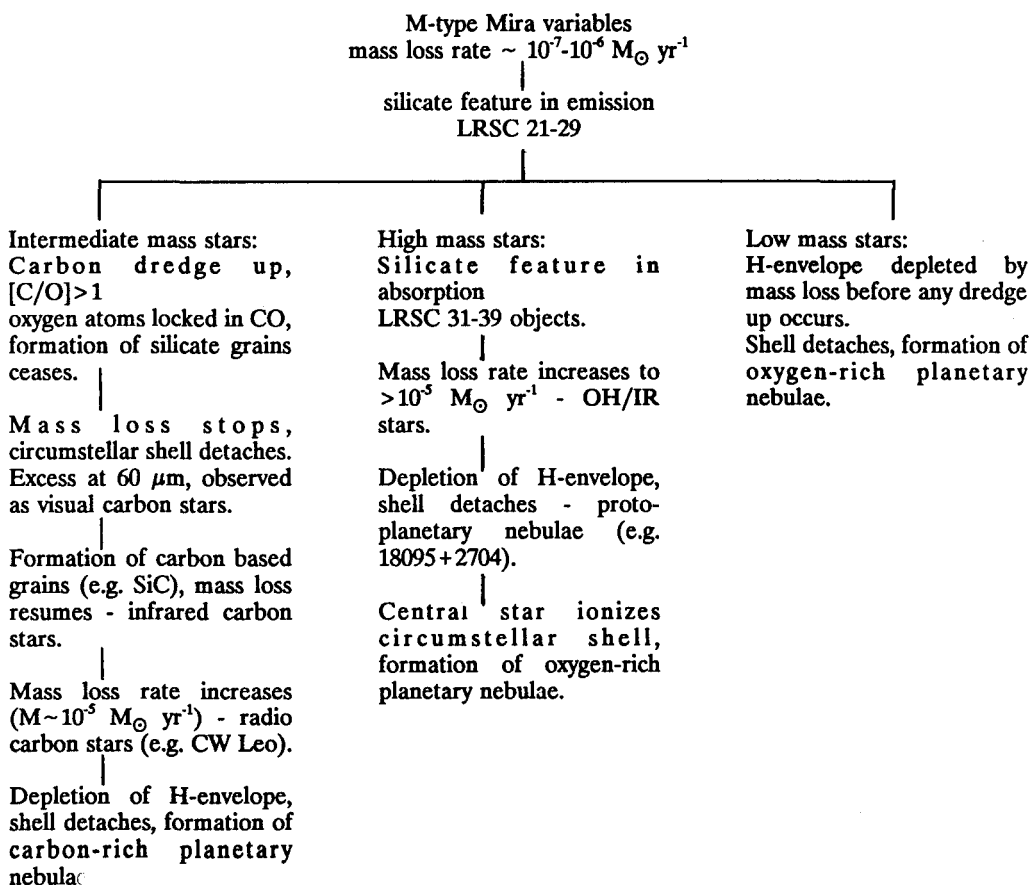
VII. Proto-planetary nebulae

The separation of AGB stars and planetary nebulae in the color-color diagram suggests that transition objects between these two phases of evolutionary phases can be discovered by observing *IRAS* objects which occupy the area in the color-color diagram between these two groups. A number of objects showing double-peak energy distributions have been found (Parthasarathy and Pottasch 1987; Hrivnak, Kwok, and Volk 1988). Such energy distributions can be explained by the dispersal of the circumstellar envelope and the emergence of light from the central star as the optical depth of the envelope declines.

VIII. Conclusions

The concept of AGB stars evolving from M to S to C has been entrenched since the early days of spectral classifications. Recent photometric and spectroscopic observations from the *IRAS* satellite suggest that all AGB stars start as mass-losing M stars; some of which remain oxygen-rich while others become carbon rich. One possible parameter which may determine what branch a star will take is the initial mass. For a low mass star, the hydrogen envelope is small and the entire envelope may be lost before any dredge up occurs. For high mass stars, thermal pulse does not begin until the stellar luminosity is very high ($\sim 3 \times 10^4 L_{\odot}$ for a $6 M_{\odot}$ star, Iben 1981). At such high luminosities, the mass loss rates will be very high and the hydrogen envelope may be totally depleted before enough carbon is dredged up to the surface. A summary of the suggested evolutionary scenario is given in Table 2.

Table 2



This work is supported by the Natural Sciences and Engineering Research Council of Canada.

References

- Chan, S.J., and Kwok, S. 1988, *Astrophys. J.*, in press.
- Bedijn, P.J. 1987, *Astron. Astrophys.*, **186**, 136.
- Castellani, V., Chieffi, A., Pulone, L., and Tornambe, A. 1985, *Astrophys. J.*, **296**, 204.
- Hrivnak, B.J., Kwok, S., and Volk, K.M. 1988, *Astrophys. J.*, in press.
- Iben, I. 1975, *Astrophys. J.*, **196**, 549.
- _____ 1981, *Astrophys. J.*, **246**, 278.
- Kwok, S. 1980, *Astrophys. J.*, **236**, 592.
- Lattanzio, J.C. 1986, *Astrophys. J.*, **311**, 708.
- MacConnell, D.J. 1988, *Astron. J.*, **96**, 354.
- Olson, F.M., Baud, B., Habing, H.J., deJong, T., Harris, S., and Pottasch, S.R. 1984, *Astrophys. J. (Letters)*, **278**, L41.
- Olofsson, H., Eriksson, K., and Gustafsson, B. 1987, *Astron. Astrophys.*, **183**, L13.
- _____ 1988, *Astron. Astrophys.*, **196**, L1.
- Parthasarathy, M., and Pottasch, S.R. 1987, *Astron. Astrophys.*, **154**, L16.
- Stephenson, C.B. 1983, *A General Catalogue of Cool Carbon Stars*, Publ. Warner and Swasey Obs., **1**, No. 4 (GCCCS).
- _____ 1976, *A General Catalogue of S Stars*, Publ. Warner and Swasey Obs., **2**, No. 2.
- Pottasch, S.R. *et al.* 1984, *Astron. Astrophys.*, **138**, 10.
- van der Veen, W.E.C.J., and Habing, H. 1988, *Astron. Astrophys.*, **194**, 125.
- Volk, K., and Kwok, S. 1988, *Astrophys. J.*, in press.
- Willems, F., and deJong 1988, *Astron. Astrophys.*, **196**, 173.
- Zuckerman, B., and Dyck, M. 1986, *Astrophys. J.*, **311**, 345.